Diffusion and Dynamics of Gamma-Globulin in Crowded Aqueous Solutions.

5 **AUTHORS**, INCLUDING:

Marco Grimaldo
University of Tuebingen
6 PUBLICATIONS **16** CITATIONS

SEE PROFILE

Tilo Seydel
Institut Laue-Langevin
85 PUBLICATIONS **967** CITATIONS

SEE PROFILE

Frank Schreiber
University of Tuebingen
225 PUBLICATIONS **7,349** CITATIONS

SEE PROFILE

Diffusion and Dynamics of γ-Globulin in Crowded Aqueous Solutions

Marco Grimaldo,[†,‡] Felix Roosen-Runge,[†] Fajun Zhang,[‡] Tilo Seydel,[*,†] and Frank Schreiber[‡]

[†]Institut Max von Laue − Paul Langevin (ILL), B.P.156, F-38042 Grenoble, France
[‡]Institut für Angewandte Physik, Universität Tübingen, Auf der Morgenstelle 10, D-72076 Tübingen, Germany

S *Supporting Information*

ABSTRACT: Dynamics in protein solutions is essential for both protein function and cellular processes. The hierarchical complexity of global protein diffusion, side-chain diffusion, and microscopic motions of chemical groups renders a complete understanding challenging. We present results from quasi-elastic neutron scattering on protein solutions of γ-globulin over a wide range of volume fractions. Translational and rotational diffusion can be self-consistently separated from internal motions. The global diffusion is consistent with predictions for effective spheres even though the branched molecular shape differs considerably from a colloidal sphere. The internal motions are characterized both geometrically and dynamically, suggesting a picture of methyl rotations and restricted diffusion of side chains. We show that the advent of new neutron spectrometers allows the study of current questions including the coupling of intracellular dynamics and protein function.
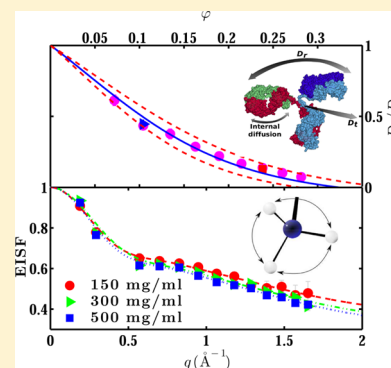
1. INTRODUCTION

Protein function in cellular processes is strongly influenced by the intracellular environment. The high volume occupancy of macromolecules of roughly 20−40%, the so-called macromolecular crowding, affects biochemical reaction rates,[1] slows diffusive transport processes, and can cause compaction of protein conformations.[2−4] Recently, several publications have focused on protein dynamics in living cells,[5] addressing diffusion of proteins in the nucleoplasm,[6] in the mitochondrial lumen,[7] and in the cytoplasm.[8−11] Generally, in vivo protein dynamics is found to be significantly slower than in dilute protein solutions.

To mimic the effect of crowding in vivo, several in vitro studies have addressed concentrated solutions of one protein (self-crowding), allowing systematic investigation of crowding effects on diffusion as well as a conceptual understanding along colloid theory.[12−15] Brownian dynamics simulations[16] indicate that a major part of the diffusional slowing in crowded protein solutions is due to hydrodynamic interactions. In this context, the short-time limit of self-diffusion is of particular interest because hydrodynamic interactions are established quasi-instantaneously even on larger length scales, while other protein interactions become relevant near the interaction time $\tau_I \approx 400$ ns for medium-sized globular proteins.[17] Recently, the protein self-diffusion on nanosecond time and nanometer length scales in aqueous solution has been found to be consistent with short-time predictions from colloid theory for the model globular protein BSA.[18]

The successful modeling of global diffusion is promising for a better understanding of protein internal dynamics on a molecular level and possible effects of crowding. Numerous studies have focused on the protein internal dynamics on the subnanosecond time scale; however, mainly in more or less hydrated powders[19−24] because in this case global diffusion does not interfere with the internal dynamics during the data analysis. Only a few of them have been performed on protein solutions[25−27] or in vivo,[28,29] but without systematically addressing the effect of crowding.

We report on a comprehensive study of diffusive dynamics in crowded aqueous γ-globulin protein solutions on a molecular length scale using quasi-elastic neutron spectroscopy. The measured spectra contain contributions from the global rotational D_r and translational D_t diffusion of the entire protein as well as from internal diffusive protein motions and the solvent water. We perform a self-consistent separation of these different contributions to quantitatively extract $D_t = D_t(\varphi)$ as well as information on the internal motions, thereby describing a wide range of volume fractions φ to reliably address dynamical effects of crowding. The results are consistent with short-time self-diffusion of the protein center of mass superimposed with geometrically confined internal diffusive motions dominated by methyl rotations and restricted side-chain motions.

We have carried out our investigation as one of the first experiments of the recently commissioned neutron back-scattering spectrometer IN16B at ILL, Grenoble, with an energy range of $-30~\mu\text{eV} \leq \hbar\omega \leq +30~\mu\text{eV}$ at a Gaussian resolution of 0.9 μeV full width at half-maximum (fwhm) and the scattering vectors $0.2~\text{Å}^{-1} \leq q \leq 1.9~\text{Å}^{-1}$. IN16B provides an unprecedentedly high neutron flux at this energy resolution and range. We have measured the native protonated proteins in heavy water (D_2O) solutions to reduce the solvent contribution

to the measured signal. In this way, the recorded quasi-elastic neutron scattering (QENS) spectra are dominated by the incoherent scattering from the hydrogen ^{1}H nuclei of the proteins. Thus, to good approximation we obtain the incoherent scattering function $S(q,\omega)$ which, for our system, is proportional to the ensemble-averaged ^{1}H-single-atom self-correlation function. Importantly, given the instrument characteristics, we unambiguously access self-diffusion and individual internal motions on nanosecond time scales and nanometer length scales.

The article is organized as follows: In the next section, we provide further details on the experiment, sample preparation, data reduction, and fits. Subsequently, we present and discuss our results regarding both the translational short-time self-diffusion $D_t(\varphi)$ of γ-globulin in aqueous solution as well as its internal molecular diffusive motions in detail. In the concluding section, we outline the statements that can presently be made and we also point out possibilities for future continuations.

2. EXPERIMENTS AND METHODS

2.1. Sample Preparation. Bovine γ-globulin was purchased from Sigma-Aldrich (purity of 99%, G5009) and used without further purification. The samples at protein concentration $c_p = m_p/V_{D_2O}$ were prepared by dissolving the protein powder with mass m_p in a volume V_{D_2O} of D_2O. After complete dissolution, the solutions were filled in double-walled aluminum cylinders with outer diameter 23 mm and a gap of 0.16 mm; the cylinders were then sealed against vacuum. The volume fraction φ occupied by the bare proteins is given by

$$\varphi = \frac{\vartheta m_p}{V_{D_2O} + \vartheta m_p} \tag{1}$$

where $\vartheta = 0.739$ mL/g is the specific volume of γ-globulin.[30] The samples were prepared to cover a φ-range of $\sim$10−28%. Using eq 1, we assume that the protein hydration shell volume does not depend on the crowding. Such small crowding effects of the hydration shell may occur,[31] but it is difficult to quantify them for γ-globulin without a separate comprehensive volumetric study. To not introduce further experimental errors, we assume that eq 1 is valid with sufficient accuracy.

2.2. Quasi-elastic Neutron Backscattering. The experiments were carried out using the newly commissioned cold neutron backscattering spectrometer IN16B at the Institut Laue-Langevin (ILL),[32] achieving a Gaussian energy resolution of 0.9 μeV fwhm. The samples were inserted in a standard Orange cryofurnace mounted inside the evacuated secondary spectrometer chamber. The instrument was used with unpolished Si(111) crystal monochromator and analyzers and a vertically position-sensitive multidetector (PSD) consisting of 16 ^{3}He detector tubes covering the scattering vector range 0.57 Å^{-1} < q < 1.94 Å^{-1}. In addition, two small-angle detectors with a slightly lower energy resolution due to a small angular deviation from backscattering were placed at q = 0.19 Å^{-1} and 0.29 Å^{-1}, respectively. The energy transfer −30 μeV < $\hbar\omega$ < 30 μeV was achieved in the so-called inverse geometry by Doppler-shifting the incident monochromatic neutrons using an AEROLAS Doppler drive operating with a sinus velocity profile with an amplitude of 75 mm and maximum velocity of 4.5 m/s. The flux at the sample was optimized by the phase space transformer (PST) chopper disk[33] carrying graphite mosaic crystals at its circumference and spinning at 7100 rpm

during the experiment, corresponding to a crystal velocity of 243 m/s. For every sample, we measured approximately 4 h at full energy range, which results in similar or better statistics than when measuring on the predecessor instrument IN16 during 24 h.

2.3. Measured Spectra and Fits, Modeling of the Contribution of D_2O. All data reductions and fits are carried out using MATLAB R2012b. We normalize the measured intensities by the incident neutron flux and detector efficiency, and we subtract the empty can signal from the protein solution spectra. The thus obtained scattering function $S(q,\omega)$ describing the protein solution spectra recorded on IN16B is modeled by the following expression:[18]

$$S(q, \omega) = \mathcal{R} \otimes \{\beta[A_0(q)\mathcal{L}_\gamma(\omega) + (1 - A_0(q))\mathcal{L}_{\gamma+\Gamma}(\omega)]$$
$$... + \beta_{D_2O}\mathcal{L}_{\gamma D_2O}(\omega)\} \tag{2}$$

Therein, $\mathcal{L}$ denotes a Lorentzian function, and the index to this symbol the respective half-width at half-maximum. $\mathcal{R}$ is the nearly perfect Gaussian resolution function of IN16B determined from the spectrum of a Vanadium standard (width 0.9 μeV fwhm). In the fit of eq 2 to the IN16B spectra, the line widths γ and Γ as well as the amplitudes β and A_0 are free to take any positive real value, and their physical meaning will become clear in the Results and Discussion section. All other parameters are fixed, including β_{D_2O} and $\mathcal{L}_{\gamma D_2O}(\omega)$, as explained further below. The spectra for the individual q-values are fitted independently, i.e., no q-dependence is imposed on the fits. In the fit algorithm, $\mathcal{R}$ is described analytically by a sum of Gaussian functions, and the convolution $\mathcal{R} \otimes \{...\}$ is carried out analytically using Voigt functions built from $\mathcal{R}$ and $\mathcal{L}_{\{...\}}$. On the energy range $2\Delta\omega_{max}$ accessible by IN16B, the line broadening $\mathcal{L}_{\gamma D_2O}(\omega)$ due to the D_2O solvent contribution is not flat even though the half-width at half-maximum (HWHM) $\Delta\omega$ of the D_2O spectra with intensity $I_{D_2O}(\omega)$ is bigger than $\Delta\omega_{max}$. This may result in systematic uncertainties when subtracting the rescaled D_2O spectra $I_{D_2O}^{(\varphi)}(q,\omega) = (1 - \varphi) I_{D_2O}(q,\omega)$ from the spectra of the solutions at protein volume fraction φ. To self-consistently quantify the contribution of heavy water and simultaneously reduce systematic errors, we combine D_2O measurements performed at the cold neutron time-of-flight spectrometer IN6 (ILL) and at the cold neutron backscattering spectrometer IN16B (see also Supporting Information). IN6 has the advantage of a substantially larger energy range (at the expense of energy resolution) and is thus better suited to measure the fast dynamics of D_2O and model the QENS line width γ_{D_2O} as a function of q^2. The D_2O spectra measured at IN16B and rescaled according to φ are then used to fit the amplitude β_{D_2O} of the modeled D_2O contribution $\mathcal{L}_{\gamma D_2O}(\omega)$. Finally, $\beta_{D_2O}(\omega)\mathcal{L}_{\gamma D_2O}$ is added as a fixed term to eq 2, thus eliminating unnecessary free parameters in the fit.

2.4. Diffusion Coefficients: Separation of Rotational and Translational Diffusion. The proteins in solution undergo both translational center-of-mass diffusion and rotational diffusion, which are convoluted in the measured signal, resulting in the observable apparent diffusion coefficient D. The fit parameter γ in eq 2 is associated with this apparent diffusion coefficient D of the proteins, as explained further in the following section. To compare the experimental results with existing theories, the extraction of the translational part D_t and

the rotational part D_r from D is performed following the method in ref 18 based on an implicit relation $D(\varphi) = D(D_r(\varphi), D_t(\varphi))$ (see also Supporting Information). For this separation, we employ the colloid model for $D_r = D_r(\varphi)$. At the high q explored in our experiment, rotational diffusion contributes to a q-independent apparent diffusion coefficient,[18] which enhances the robustness of the separation. The dilute limit translational $D_0 = 3.29$ Å^2/ns and rotational $D_{r,0} = 0.7 \times 10^{-3}$ ns^{-1} diffusion coefficients, as well as the molecular volume $V_p = 251$ nm^3, are calculated via HYDROPRO[34] using the crystal structure of murine immunuglobulin G (IgG) that can be identified with the γ-globulin in our samples except for some negligible amount of other immunoglobulins.[35] D_0 is in very good agreement with recent DLS measurements by Wang et al.[36] yielding $R_h = 55$ Å, i.e., $D_0 = 3.3$ Å^2/ns in D$_2$O at $T = 295$ K.

3. RESULTS AND DISCUSSION

**3.1. Neutron Spectra.** The inset of Figure 1 depicts a typical QENS spectrum $S(q,\omega)$ (red circles) which can be well
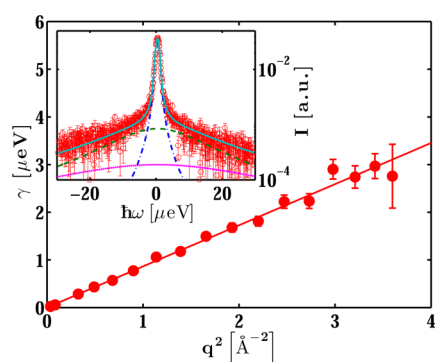
Figure 1. Inset: typical $S(q,\omega)$ (red circles) recorded using cold neutron backscattering for γ-globulin in D$_2$O ($c_p = 300$ mg/mL; $T = 295$ K; individual detector at $q = 0.81$ Å^{-1}). The lines depict the Lorentzian functions $\mathcal{L}_\gamma(\omega)$ (blue dot-dashed), $\mathcal{L}_{\gamma+\Gamma}(\omega)$ (green dashed), and $\mathcal{L}_{\gamma D_2 O}(\omega)$ (magenta dotted) in eq 2. The turquoise solid line superimposed on the data is the result of the complete fit using eq 2. Main figure: fitted γ (red circles) versus q^2 for the full accessible q-range. The fit $\gamma = Dq^2$ (solid red line) indicates a simple Brownian diffusive behavior. The fit range is restricted to $q^2 < 1.5$ Å^{-2} (see text).

described by eq 2 (turquoise solid line). Here, the sum of three Lorentzian functions $\mathcal{L}(\omega)$ models a slower process with line broadening γ (blue dot-dashed line), a convoluted faster process with line broadening $\gamma + \Gamma$ (green dashed line), and the solvent contribution (magenta dotted line) with fixed values for both width γ_{D_2O} and intensity β_{D_2O} (see the previous section for details on the data reduction and fits; see the Supporting Information for further example spectra). $A_0(q)$ in eq 2 is identified with the elastic incoherent structure factor (EISF). We emphasize that the processes occur on well-separated time scales, such that it is possible to distinguish between the different components in the measured spectra.

For the slower process, the relationship $\gamma = Dq^2$ (Figure 1) indicates a simple diffusion with apparent diffusion coefficient $D(\varphi)$. Note that the slight deviation from this law for higher q-values is presumably due to a weakened signal once the width of $S(q,\omega)$ exceeds the accessible energy range for higher q-values. To avoid artifacts, we restrict the fits for $D(\varphi)$ to $q^2 < 1.5$ Å^{-2}, where $\gamma = Dq^2$ clearly holds for all samples.
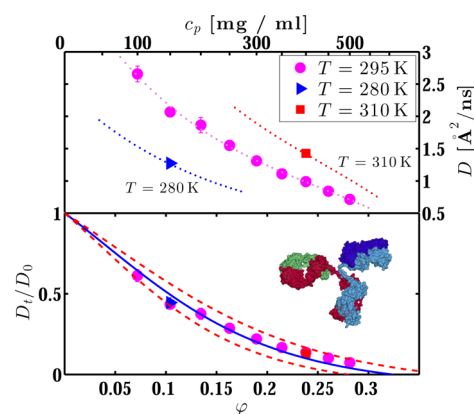
Figure 2. Apparent diffusion coefficient D (upper panel) and reduced translational short-time diffusion coefficient D_t/D_0 (lower panel) as a function of the protein volume fraction φ. The symbols represent the experimental data recorded at $T = 295$ K (circles), $T = 280$ K (triangles), and $T = 310$ K (squares). In the upper plot, the lines are guides to the eye (dotted). In the lower plot, the solid blue line depicts the normalized translational short-time self-diffusion from colloid theory for hard spheres.[37] The dashed red lines indicate the colloid model for a 5% relative error on R_h/R. When not visible, the experimental error bars are smaller than the symbols. The protein structure was rendered using VMD.

The apparent diffusion coefficients $D(\varphi)$ are shown in the upper part of Figure 2. The increase of φ causes a significant decrease of $D(\varphi)$, consistent with previous studies on bovine serum albumin.[18,38] The lower and higher temperature is used to test the robustness of the analysis against temperature effects, which might cause protein dynamics to exceed the accessible energy range.

3.2. Rotational and Translational Diffusion of the Proteins. The normalized translational self-diffusion coefficients $D_t(\varphi)/D_0$ (Figure 2) are determined by the established deconvolution scheme[18] based on the implicit relation $D(\varphi) = D(D_r(\varphi), D_t(\varphi))$ (see the preceding section on Experiments and Methods). Within this scheme, the proteins are modeled by effective spheres with the hydrodynamic radius of protein monomers as calculated by HYDROPRO.[34] The theoretical prediction for the translational short-time self-diffusion coefficients of these effective spheres (blue solid line) are in very good agreement with the experimental values for γ-globulin (symbols) (Figure 2, bottom). Thus, the slower process can be identified and accurately modeled with the global self-diffusion of protein molecules. We stress that the dilute limit diffusion coefficient enters only for the normalization to D_0 in Figure 2 and for the rather robust separation of the translational and rotational diffusion. Therefore, an uncertainty in D_0 will not alter the observed trend.

We point out that the data measured at $T = 280$ K (blue triangle) and $T = 310$ K (red square) are perfectly consistent with those measured at $T = 295$ K (circles), thus confirming that the effect of crowding is largely temperature-independent. To consolidate the assumption of a mainly monomeric solution, we repeated the procedure for a hypothetical dimer of γ-globulin (see also Supporting Information). The resulting $D_t(\varphi)/D_0$ from dimers is not consistent with theoretical predictions, suggesting that the data analysis based on monomers is suitable, at least at nanosecond time and nanometer length scales.

We remark that the real protein shape specified by a crystal structure enters the analysis at only two points: first, for the calculation of the hydrodynamic radii with HYDROPRO and, second, for the calculation of the radial distribution function of hydrogen with respect to the protein center of mass (see the previous section on Experiments and methods).

3.3. Internal Diffusive Molecular Motions. The faster process observed in the neutron spectra (eq 2) can be characterized both geometrically via the EISF $A_0(q)$ and dynamically via the line broadening Γ. The EISF provides information on the geometry of dynamical confinement of the hydrogen atoms within a protein molecule. Several theoretical models addressing confined diffusion provide analytical expressions for the EISF.[39−41] The most frequently used models describe either the diffusion of a particle within an impermeable sphere or a jump diffusion between two or three definite sites.[25] The experimental EISF is most probably a rather complicated superposition of several diffusion mechanisms. Therefore, regarding all discussion in this subsection, we stress that the present modeling is far from final, and in what follows we chose one out of possibly various alternative approaches. We also note that the restricted dynamic range on which the spectra were recorded (i.e., the maximum energy transfer and energy resolution limits of IN16B) may pose systematic limitations to the conclusions on the internal motions. Furthermore, we emphasize that the observable quantity in our experiment is the self-dynamics of the prevailing hydrogen atoms. Using neutron backscattering, we observe uncorrelated individual fluctuations of protein subunits on the nanometer length scale, e.g., the motions of methyl groups and other amino acid residues. Therefore, as opposed to neutron spin−echo experiments, our incoherent scattering experiment is not sensitive to correlated long-range interdomain fluctuations within the proteins.

For the sake of simplicity, we assume the protein to be a dynamically heterogeneous system, so that the EISF is expected to be a simple sum of weighted contributions.[41,42] It is well-known that a large part of the hydrogen atoms within a protein form methyl groups ($-CH_3$), where the three hydrogens, located at an average distance $a_M = 3^{1/2} \cdot 0.99\ \text{Å} \simeq 1.715\ \text{Å}$ from each other, perform 120°-jumps around the 3-fold axis.[43,44] Thus, one expects a significant component of the EISF due to three-sites jump diffusion:[25,44,45] $A_{3\text{-jump}}(q) = 1/3[1 + 2 j_0(qa)]$, where $j_0(x) = \sin(x)/x$ and $a \equiv a_M$ denotes the jump-distance of the atom. As a second component we choose the EISF of an atom diffusing freely within an impermeable sphere of radius R without any a priori physical interpretation:[39,45] $A_{\text{sphere}}(q) = |3\, j_1(qR)/(qR)|^2$, where $j_1(x)$ is the first order spherical Bessel function of the first kind. The components are assumed to be uncorrelated such that the total EISF is modeled as

$$A_0(q) = P + (1 - P)[\Phi A_{3\text{-jump}}(q) + (1 - \Phi)A_{\text{sphere}}(q)] \tag{3}$$

Here, Φ is the fraction of hydrogen atoms undergoing three-sites jump diffusion, and $(1 - \Phi)$ is the fraction of hydrogens diffusing in an impermeable sphere. P represents the fraction of hydrogen atoms that appear fixed on the accessible time-scale.[46] Figure 3 shows the EISF as a function of q for three different c_p (symbols) along with fits using eq 3 (lines).

The parameters obtained from the fit are listed in the Supporting Information. Within the error, they are constant and have error-weighted average values of $R = 6.7 \pm 0.27\ \text{Å}$, $P =$
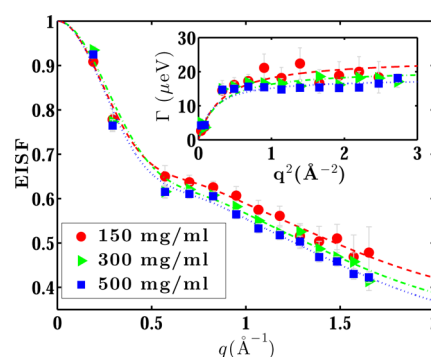
Figure 3. Main figure: elastic incoherent structure factor as a function of q for three γ-globulin concentrations (symbols). The lines are the fits by eq 3. Inset: Γ as a function of q^2 for three protein concentrations. The symbols are the experimental data, and the lines are the fits with eq 4.
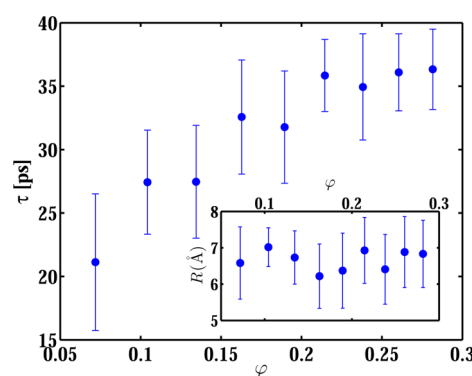
Figure 4. Main figure: fit results for the residence time τ associated with the internal molecular motion of the proteins in terms of the jump diffusion model (eq 4) as a function of the protein volume fraction φ in the aqueous solution. Inset: fit result for the radius R of the impermeable sphere associated with the protein side-chain motions in terms of the model for the EISF (eq 3) as a function of the protein volume fraction φ.

0.28 ± 0.02, and $\Phi = 0.55 \pm 0.02$. The fit results for R are also depicted in the inset of Figure 4. These results are comparable to analogous parameters calculated in other studies.[25,26,47] From a rough estimation of the amount of CH_3 in γ-globulin we obtain $\Phi = 0.22$. The fit for this scenario of a fixed Φ (see Supporting Information) is less good compared to that of the situation with a free parameter Φ. This is reasonable because the EISF does not allow the extraction of the number fractions of the different atoms corresponding to different internal diffusive processes on an absolute scale because of the restricted dynamic window on which the diffusion is sampled.

An increased thermal stability of proteins under crowding conditions has been reported in previous studies.[48−50] However, the anticipated effect of crowding on the thermal stability is small.[2] It is therefore not surprising that the fit parameters in the EISF, characterizing the geometrical confinement of internal motions, do not significantly vary with the protein concentration in our experiment. In particular, Stagg et al.[2] report an isotropic compaction of proteins of about 0.3% in the radius of gyration R_g in highly crowded solutions. The absence of a significant change of the geometry to which the internal motions are confined, as reflected by the radius R in the EISF (Figure 4, inset), is consistent with such a small change in R_g.

In addition to the geometrical information via the EISF, Γ provides a dynamical signature of internal motions that occur in the time window defined by the resolution and the energy range of the instrument. For the three-sites jump-diffusion modeling methyl rotations, the residence time is of the order of 10^{-10} s, corresponding to a HWHM of the order of 100 μeV, well above the energy range of IN16B. Hence, the resulting signal is expected to be essentially flat[44] and will thus not contribute to Γ. For confined diffusion in a sphere, the dynamical signature should be present in Γ. In the first approximation, we can use an expression for unrestricted jump-diffusion to fit our data. In the absence of a detailed microscopic dynamical picture, for simplicity we apply the model of Singwi and Sjölander[26,40,51]

$$\Gamma = \frac{D_{jump}q^2}{1 + D_{jump}q^2\tau} \tag{4}$$

where τ denotes the residence time before a jump and D_{jump} is the jump-diffusion coefficient. The inset of Figure 3 shows Γ as a function of q^2 for three c_p. The lines are the fits by eq 4. The fitted D_{jump} results in values around 150 Å²/ns, while $\tau(\varphi)$ seems to follow an asymptotic behavior, monotonically increasing with c_p from $\tau \sim 20$ ps at $c_p = 100$ mg/mL to $\tau \sim 40$ ps at $c_p = 500$ mg/mL (see Figure 4, main part). Within the errorbars, these values are consistent also with those obtained by fitting the data with the comparable model for unrestricted jump-diffusion by Hall and Ross.[52] However, at present our theoretical understanding is not yet sufficient to fully validate the picture of jump diffusion or a related model. Molecular dynamics simulations may in the future resolve this issue in combination with QENS experiments along the framework presented in this article.

From the geometrical and dynamical information on the internal motions, we obtain the picture of an insignificant change of the geometry of the confined motion with increasing crowding. By contrast, those hydrogen relaxations sampled on an excitation scale of some 10 μeV are subject to an increased residence time at higher crowding. Because crowding shifts the thermodynamic equilibrium of proteins toward a more folded state,[2,53] a small effect of crowding on the internal molecular fluctuations of proteins may be expected. It has been hypothesized that the structuring effect of water plays a role in this stabilization.[53] The trend in the residence time τ in terms of the jump diffusion model might be related to this stabilization. Perez et al.[25] have shown that internal motions in fully dissolved proteins are faster than those in hydrated protein powders in the case of lysozyme and myoglobin. Because we use D_2O as solvent water, we assume that the contribution of the hydration shell itself to our measured signal is small, but we cannot yet make a conclusive statement on the role of the hydration shell water on the internal dynamics of γ-globulin. Nevertheless, the slower internal diffusion with increasing crowding observed in our experiment would be consistent with the trend toward even slower diffusion in hydrated powders, the latter being the "ultimately crowded" solution.

3.4. Further Discussion. The successful and self-consistent separation of global and internal motions using colloidal modeling of the protein is a central result of this study because it not only describes the protein diffusion very well but also allows for reliable access of the convoluted internal dynamics, which is promising for future applications of neutron backscattering. In this context, several questions deserve further discussion.

Protein solutions can not, in general, be considered as purely monodisperse solutions of monomers, but might also contain oligomers and clusters. Although previous studies have reported oligomerization of γ-globulin[54,55] at concentrations up to ~150 mg/mL, our data accessing high protein concentrations are fully consistent with a monomeric description. A tentative separation of motions using dimers results in inconsistent diffusion coefficients, indicating that oligomerization has a negligible effect at these short time scales. Large aggregates would not cause a quasi-elastic signal measurable by IN16B but contribute only to the amplitude of the elastic line. Small oligomers would lead to an additional contribution to the quasi-elastic broadening. None of these effects is visible in our data. In addition, the good agreement of the experimental $D_t(\varphi)$ with the theoretical prediction from colloid theory based on the assumption of γ-globulin monomers is consistent with the picture that all our samples are predominantly monomeric protein solutions. We remark, however, that we cannot rule out the presence of aggregates in some form. We also note that oligomerization or aggregation may depend on the type of antibody protein, and we emphasize that our samples are not monoclonal.

Proteins can have different conformations[56] that coexist in solution or are switched because of environmental factors. In particular, pH-induced conformational changes of the protein can constitute a limitation to the applicability of colloid models to protein solutions.[57] Nevertheless, over the investigated concentration range, the pH is expected to be sufficiently constant because of self-buffering ensuring a substantially unchanged protein conformation for our samples.

The strongly anisotropic shape of γ-globulin inspires the question whether interdomain motions of the three branches of the protein may interfere with our analysis. In this context, we remark that on the observation time scale of our experiment, the measured D values correspond to a mean-squared displacement of the proteins by a few angstroms. This length scale is much smaller than the radius of γ-globulin. Also, $D_{r,0}$ of γ-globulin corresponds to a root mean-squared rotational displacement[58] of about 3°. Therefore, it is reasonable that the influence of the strongly branched shape of the protein does not lead to a deviation from the colloid hard-sphere model in the short-time limit. Stronger deviations may be expected to become significant at longer times. Even though the interdomain motions are not visible in our experiment, we note that they may be affected by the change in the hydrodynamic interactions due to crowding.

The large energy range of the new backscattering spectrometer IN16B allows access to information on dynamics in the subnanosecond to nanosecond time scale, which represents methodological challenges. Within this time window, water motions become visible and the data analysis has to be reliably set up based on a physical picture. In our case, the scattering of the sample cylinder and instrumental background has been directly subtracted using a background measurement. The water contribution has been removed by a novel method employing results on D_2O from the time-of-flight spectrometer IN6 (see the section on Experiments and Methods). With this method, we minimize effects of the water scattering on the determination of Γ.

Concerning the fit procedure, we emphasize that both γ and Γ in eq 2 are left completely free during the fit. The final result

is very robust against variation of the initial values, meaning that both components are present and well-separated. The second component $\mathcal{L}_\Gamma(\omega)$ clearly does not follow a $\Gamma \propto q^2$ behavior, indicating *no* free diffusion, but diffusion in a confinement of some form. The data are at this stage not sufficient to further distinguish between different types of confined diffusion arising from processes such as rotational jump-diffusion of the methyl and amine groups and diffusion of the tethered side chains of the amino acids, as well as confined diffusion of the hydration water. Nevertheless, the overall procedure is promising for allowing such distinction also in view of future instrumental developments aimed at increasing the neutron flux to the sample. Further progress in the analysis of the component $\mathcal{L}_\Gamma(\omega)$ may be possible by comparison to molecular dynamics (MD) simulations and a complementary study on a wider energy range.

4. CONCLUSIONS AND OUTLOOK

Using quasi-elastic neutron backscattering, we have successfully accessed self-diffusion and internal dynamics in aqueous solutions of γ-globulin on subnanosecond to nanosecond time and nanometer length scales. The study presents the results of one of the first experiments conducted at the newly commissioned backscattering spectrometer IN16B at the Institut Laue-Langevin. To minimize systematic errors, the data analysis has been reviewed carefully and extended by a newly developed procedure to account for solvent contributions. Because of the high data quality, it was possible to apply a self-consistent separation framework for the global translational and rotational diffusion and internal motions. The global diffusion is described with good agreement by predictions for effective spheres with the hydrodynamic radius of the strongly nonspherical protein monomers. The internal motions are characterized both geometrically and dynamically and consist of several contributions, including jump-like rotation of chemical end groups and confined diffusion. The dynamical signature indicates a slowing of the internal dynamics because of crowding, which might be related to the thermal stabilization of the protein conformation. Although the modeling of the internal diffusive motions is certainly far from complete, the presented framework allows for future experimental studies with various perspectives and, in connection with accompanying instrumental, theoretical, and computational advances, is promising for a comprehensive understanding of the hierarchical and complex dynamics in protein solutions. In the future, it will also be of interest to carry out a comparative study of internal fluctuations of a hydrated protein powder of γ-globulin to compare with the internal fluctuations observed on the proteins in solution.

■ ASSOCIATED CONTENT

ⓢ Supporting Information

Details on the separation of rotational and translational diffusion and results of the separation assuming dimers in solution; radial distribution of hydrogen atoms of IgG monomers, dimers, and BSA; summary of fit results of the EISF and Γ; details on the treatment of the contribution of heavy water; and additional example spectra. This material is available free of charge via the Internet at http://pubs.acs.org.

■ AUTHOR INFORMATION

Corresponding Author

*E-mail: seydel@ill.eu.

Notes

The authors declare no competing financial interest.

■ ACKNOWLEDGMENTS

■ REFERENCES

(1) Ellis, R. Macromolecular Crowding: An Important but Neglected Aspect of the Intracellular Environment. *Curr. Opin. Struct. Biol.* **2001**, *11*, 114−119.

(2) Stagg, L.; Zhang, S.; Cheung, M.; P, W. Molecular Crowding Enhances Native Structure and Stability of α/β Protein Flavodoxin. *Proc. Natl. Acad. Sci. U.S.A* **2007**, *104*, 18976−18981.

(3) Hong, J.; Gierasch, L. Macromolecular Crowding Remodels the Energy Landscape of a Protein by Favoring a More Compact Unfolded State. *J. Am. Chem. Soc.* **2010**, *132*, 10445−10452.

(4) Dhar, A.; Samiotakis, A.; Ebbinghaus, S.; Nienhaus, L.; Homouz, D.; Gruebele, M.; Cheung, M. Structure, Function, and Folding of Phosphoglycerate Kinase Are Strongly Perturbed by Macromolecular Crowding. *Proc. Nat. Acad. Sci. U.S.A.* **2010**, *107*, 17586−17591.

(5) Lippincott-Schwartz, J.; Snapp, E.; Kenworthy, A. Studying Protein Dynamics in Living Cells. *Nat. Rev. Mol. Cell Biol.* **2001**, *2*, 444−456.

(6) Phair, R.; Misteli, T. High Mobility of Proteins in the Mammalian Cell Nucleus. *Nature* **2000**, *404*, 604−609.

(7) Partikian, A.; Ölveczky, B.; Swaminathan, R.; Li, Y.; Verkman, A. Rapid Diffusion of Green Fluorescent Protein in the Mitochondrial Matrix. *J. Cell Biol.* **1998**, *140*, 821−829.

(8) Swaminathan, R.; Hoang, C.; Verkman, A. Photobleaching Recovery and Anisotropy Decay of Green Fluorescent Protein GFP-S65T in Solution and Cells: Cytoplasmic Viscosity Probed by Green Fluorescent Protein Translational and Rotational Diffusion. *Biophys. J.* **1997**, *72*, 1900−1907.

(9) Wojcieszyn, J.; Schlegel, R.; Wu, E.-S.; Jacobson, K. Diffusion of Injected Macromolecules within the Cytoplasm of Living Cells. *Proc. Natl. Acad. Sci. U.S.A* **1981**, *78*, 4407−4410.

(10) Arrio-Dupont, M.; Foucault, G.; Vacher, M.; Devaux, P.; Cribier, S. Translational Diffusion of Globular Proteins in the Cytoplasm of Cultured Muscle Cells. *Biophys. J.* **2000**, *78*, 901−907.

(11) Verkman, A. Solute and Macromolecule Diffusion in Cellular Aqueous Compartments. *Trends Biochem. Sci.* **2002**, *27*, 27−33.

(12) Longeville, S.; Doster, W.; Kali, G. Myoglobin in Crowded Solutions: Structure and Diffusion. *Chem. Phys.* **2003**, *292*, 413−424.

(13) Doster, W.; Longeville, S. Microscopic Diffusion and Hydrodynamic Interactions of Hemoglobin in Red Blood Cells. *Biophys. J.* **2007**, *93*, 1360−1368.

(14) Heinen, M.; Zanini, F.; Roosen-Runge, F.; Fedunova, D.; Zhang, F.; Hennig, M.; Seydel, T.; Schweins, R.; Sztucki, M.; Antalik, M.; Schreiber, F.; Nägele, G. Viscosity and Diffusion: Crowding and Salt Effects in Protein Solutions. *Soft Matter* **2012**, *8*, 1404−1419.

(15) Nesmelova, I.; Skirda, V.; Fedotov, V. Generalized Concentration Dependence of Globular Protein Self-diffusion Coefficients in Aqueous Solutions. *Biopolymers* **2002**, *63*, 132−140.

(16) Ando, T.; Skolnick, J. Crowding and Hydrodynamic Interactions Likely Dominate in Vivo Macromolecular Motion. *Proc. Natl. Acad. Sci. U.S.A* **2010**, *107*, 18457−18462.

(17) Banchio, A.; Nägele, G. Short-Time Transport Properties in Dense Suspensions: From Neutral to Charge-Stabilized Colloidal Spheres. *J. Chem. Phys.* **2008**, *128*, 104903.

(18) Roosen-Runge, F.; Hennig, M.; Zhang, F.; Jacobs, R.; Sztucki, M.; Schober, H.; Seydel, T.; Schreiber, F. Protein Self-Diffusion in Crowded Solutions. *Proc. Natl. Acad. Sci. U.S.A.* **2011**, *108*, 11815−11820.

(19) Zaccai, G. How Soft Is a Protein? A Protein Dynamics Force Constant Measured by Neutron Scattering. *Science* **2000**, *288*, 1604−1607.

(20) Doster, W.; Cusack, S.; Petry, W. Dynamical Transition of Myoglobin Revealed by Inelastic Neutron Scattering. *Nature* **1989**, *337*, 754−756.

(21) Cornicchi, E.; Marconi, M.; Onori, G.; Paciaroni, A. Controlling the Protein Dynamical Transition with Sugar-Based Bioprotectant Matrices: A Neutron Scattering Study. *Biophys. J.* **2006**, *91*, 289−297.

(22) Paciaroni, A.; Cinelli, S.; Onori, G. Effect of the Environment on the Protein Dynamical Transition: A Neutron Scattering Study. *Biophys. J.* **2002**, *83*, 1157−1164.

(23) Paciaroni, A.; Cornicchi, E.; Francesco, A.; Marconi, M.; Onori, G. Conditioning Action of the Environment on the Protein Dynamics Studied Through Elastic Neutron Scattering. *European Biophys. J.* **2006**, *35*, 591−599.

(24) Chen, S.-H.; Liu, L.; Fratini, E.; Baglioni, P.; Faraone, A.; Mamontov, E. Observation of Fragile-to-Strong Dynamic Crossover in Protein Hydration Water. *Proc. Natl. Acad. Sci. U.S.A.* **2006**, *103*, 9012−9016.

(25) Perez, J.; Zanotti, J.; Durand, D. Evolution of the Internal Dynamics of Two Globular Proteins From Dry Powder to Solution. *Biophys. J.* **1999**, *77*, 454−469.

(26) Stadler, A.; Digel, I.; Embs, J.; Unruh, T.; Tehei, M.; Zaccai, G.; Büldt, G.; Artmann, G. From Powder to Solution: Hydration Dependence of Human Hemoglobin Dynamics Correlated to Body Temperature. *Biophys. J.* **2009**, *96*, 5073−5081.

(27) Biehl, R.; Hoffmann, B.; Monkenbusch, M.; Falus, P.; Préost, S.; Merkel, R.; Richter, D. Direct Observation of Correlated Interdomain Motion in Alcohol Dehydrogenase. *Phys. Rev. Lett.* **2008**, *101*, 138102.

(28) Stadler, A.; Digel, I.; Artmann, G.; Embs, J.; Zaccai, G.; Büldt, G. Hemoglobin Dynamics in Red Blood Cells: Correlation to Body Temperature. *Biophys. J.* **2008**, *95*, 5449−5461.

(29) Jasnin, M.; Moulin, M.; Haertlein, M.; Zaccai, G.; Tehei, M. In Vivo Measurement of Internal and Global Macromolecular Motions in *Escherichia coli*. *Biophys. J.* **2008**, *95*, 857−864.

(30) Jøssang, T.; Feder, J.; Rosenqvist, E. Photon Correlation Spectroscopy of Human IgG. *J. Protein Chem.* **1988**, *7*, 165−171.

(31) Murphy, L.; Matubayasi, N.; Payne, V.; Levy, R. Protein Hydration and Unfolding Insights from Experimental Partial Specific Volumes and Unfolded Protein Models. *Folding Des.* **1998**, *3*, 105−118.

(32) Frick, B.; Mamontov, E.; Eijck, L. V.; Seydel, T. Recent Backscattering Instrument Developments at the ILL and SNS. *Z. Phys. Chem. (Muenchen, Ger.)* **2010**, *224*, 33−60.

(33) Hennig, M.; Frick, B.; Seydel, T. Optimum Velocity of a Phase-Space Transformer for Cold-Neutron Backscattering Spectroscopy. *J. Appl. Crystallogr.* **2011**, *44*, 467−472.

(34) Ortega, A.; Amorós, D.; García De La Torre, J. Prediction of Hydrodynamic and Other Solution Properties of Rigid Proteins From Atomic- and Residue-Level Models. *Biophys. J.* **2011**, *101*, 892−898.

(35) Harris, L.; Larson, S.; Hasel, K.; McPherson, A. Refined Structure of an Intact IgG2a Monoclonal Antibody. *Biochemistry* **1997**, *36*, 1581−1597.

(36) Wang, Y.; Lomakin, A.; Latypov, R.; Laubach, J.; Hideshima, T.; Richardson, P.; Munshi, N.; Anderson, K.; Benedek, G. Phase Transitions in Human IgG Solutions. *J. Chem. Phys.* **2013**, *139*, 121904.

(37) Tokuyama, M.; Oppenheim, I. Dynamics of Hard-Sphere Suspensions. *Phys. Rev. E: Stat., Nonlinear, Soft Matter Phys.* **1994**, *50*, 16−19.

(38) Roosen-Runge, F.; Hennig, M.; Seydel, T.; Zhang, F.; Skoda, M.; Zorn, S.; Jacobs, R.; Maccarini, M.; Fouquet, P.; Schreiber, F. Protein Diffusion in Crowded Electrolyte Solutions. *BBA-Proteins Proteom.* **2010**, *1804*, 68−75.

(39) Volino, F.; Dianoux, A. Neutron Incoherent Scattering Law for Diffusion in a Potential of Spherical Symmetry: General Formalism and Application to Diffusion Inside a Sphere. *Mol. Phys.* **1980**, *41*, 271−279.

(40) Bée, M. *Quasielastic Neutron Scattering*; Adam Hilger, Bristol, 1988.

(41) Bicout, D. Influence of Environment Fluctuations on Incoherent Neutron Scattering Functions. *Phys. Rev. E: Stat., Nonlinear, Soft Matter Phys.* **2001**, *64*, 011910.

(42) Bicout, D.. Incoherent Neutron Scattering Functions for Combined Dynamics.*Proceedings of the ILL Millennium Symposium and European User Meeting*, Grenoble, France, April 6−7, 2001.

(43) Fitter, J. Confined Molecular Motions of Globular Proteins Studied in Powder Samples and in Solution. *J. Phys. IV* **2000**, *10*, 265−270.

(44) Bée, M. A Physical Insight into the Elastic Incoherent Structure Factor. *Phys. B (Amsterdam, Neth.)* **1992**, *182*, 323−336.

(45) Damay, P.; Leclercq, F. Diffusion Quasiélastique De Neutrons; Étude Des Mouvements Localisés. *J. Phys. IV* **2000**, *10*, Pr1-105−Pr1-129.

(46) Bellissent-Funel, M.-C.; Teixeira, J.; Bradley, K.; Chen, S. Dynamics of Hydration Water in Protein. *J. Phys. I* **1992**, *2*, 995−1001.

(47) Bu, Z.; Neumann, D.; Lee, S.-H.; Brown, C.; Engelman, D.; Han, C. A View of Dynamics Changes in the Molten Globule Native Folding Step by Quasielastic Neutron Scattering. *J. Mol. Biol.* **2000**, *301*, 525−536.

(48) Makowski, L.; Rodi, D.; Mandava, S.; Minh, D.; Gore, D.; Fischetti, R. Molecular Crowding Inhibits Intramolecular Breathing Motions in Proteins. *J. Mol. Biol.* **2008**, *375*, 529−546.

(49) Cheung, M.; Klimov, D.; Thirumalai, D. Molecular Crowding Enhances Native State Stability and Refolding Rates of Globular Proteins. *Proc. Natl. Acad. Sci. U.S.A.* **2005**, *102*, 4753−4758.

(50) Minh, D.; Chang, C.; Trylska, J.; Tozzini, V.; McCammon, J. The Influence of Macromolecular Crowding on HIV-1 Protease Internal Dynamics. *J. Am. Chem. Soc.* **2006**, *128*, 6006−6007.

(51) Singwi, K.; Sjölander, A. Diffusive Motions in Water and Cold Neutron Scattering. *Phys. Rev.* **1960**, *119*, 863−871.

(52) Hall, P.; Ross, D. Incoherent Neutron Scattering Functions for Random Jump Diffusion in Bounded and Infinite Media. *Mol. Phys.* **1981**, *42*, 673−682.

(53) Politi, R.; Harries, D. Enthalpically Driven Peptide Stabilization by Protective Osmolytes. *Chem. Commun. (Cambridge, U.K.)* **2010**, *46*, 6449−6451.

(54) Lilyestrom, W.; Yadav, S.; Shire, S.; Scherer, T. Monoclonal Antibody Self-Association, Cluster Formation, and Rheology at High Concentrations. *J. Phys. Chem. B* **2013**, *117*, 6373−6384.

(55) Yearley, E.; Godfrin, P.; Perevozchikova, T.; Zhang, H.; Falus, P.; Porcar, L.; Nagao, M.; Curtis, J.; Gawande, P.; Taing, R.; Zarraga, I.; Wagner, N.; Liu, Y. Observation of Small Cluster Formation in Concentrated Monoclonal Antibody Solutions and its Implications to Solution Viscosity. *Biophys. J.* **2014**, *106*, 1763−1770.

(56) Lilyestrom, W.; Shire, S.; Scherer, T. Influence of the Cosolute Environment on IgG Solution Structure Analyzed by Small Angle X-Ray Scattering. *J. Phys. Chem. B* **2012**, *116*, 9611−9618.

(57) Sarangapani, P.; Hudson, S.; Migler, K.; Pathak, J. The Limitations of an Exclusively Colloidal View of Protein Solution Hydrodynamics and Rheology. *Biophys. J.* **2013**, *105*, 2418−2426.

(58) Dhont, J. *An Introduction to Dynamics of Colloids*; Elsevier: Amsterdam, 1996.